Mechanical Systems and Signal Processing 204 (2023) 110783

Contents lists available at ScienceDirect

Mechanical Systems and Signal Processing

journal homepage: www.elsevier.com/locate/ymssp

Localizability of damage with statistical tests and sensitivity-based parameter clusters ☆

Alexander Mendler [a,b,*], Michael Döhler [b], Carlos E. Ventura [a], Laurent Mevel [b]

[a] University of British Columbia, CEME, 6250 Applied Science Lane, Vancouver BC, V6T 1Z4, Canada
[b] Univ. Gustave Eiffel, Inria, COSYS-SII, I4S, Campus de Beaulieu, 35042 Rennes, France

ARTICLE INFO

Communicated by S. Fassois

Keywords:
Structural health monitoring
Ambient vibrations
Damage localization
Statistical tests
Sensitivity
Clustering
Fisher information

ABSTRACT

Damage localization based on ambient vibration data in combination with finite element models can be challenging, in particular due to the large number of parameters in the model and noisy measurement data. Changes in different structural parameters can cause similar changes in data-driven features, and vice versa, it can be challenging to identify which parameter caused the deviation in the data. The problem is ill-conditioned and slight variations in the features, due to inherent statistical uncertainty, can lead to significant errors in the result interpretation. A possible solution is sensitivity-based statistical tests in combination with a parameter clustering approach that considers the uncertainties of data-driven features. In this context, this paper introduces the concept of damage *localizability*, and provides a framework to evaluate it based on the minimum detectable parameter changes, possible false alarms in unchanged parameters, as well as the achievable damage localization resolution. Since clustering approaches depend on user-defined hyperparameters, such as the number of clusters, the second objective of this paper is to optimize the performance of the damage localization, by adjusting the hyperparameters for clustering. A particular strength of the approach is that the analysis can be conducted based on data and a numerical model from the undamaged structure alone, making it a suitable approach to assess and to optimize the diagnosis performance before damage occurs. For proof of concept, a laboratory case study on a simply-supported steel beam is presented, where the localizability of mass changes is analyzed and optimized.

1. Introduction

Modern societies critically depend on structural and mechanical systems, such as, power plants, bridges, offshore platforms, defense systems, aircraft, and spacecraft. Some structures are located in remote locations, they are exposed to extreme natural hazards, or are operated beyond their original lifespan. To guarantee a safe operation, it is essential to supplement visual inspections with automated monitoring strategies and to assess the performance of the monitoring systems before damage occurs, ideally, before the structure is instrumented.

In civil engineering, the process of implementing an automated damage diagnosis procedure is known as structural health monitoring (SHM). Essential steps include the operational evaluation of the structure, the acquisition of system response data through permanently installed sensors, the extraction of damage-sensitive features, and the subsequent statistical evaluation [2], which is divided into detection, localization, quantification, and lifetime prognosis [3]. Vibration-based approaches based on the global

☆ A preliminary version of this paper was presented at the 21st IFAC World Congress, July 12–17, 2019, Berlin, Germany [1].

* Corresponding author.
E-mail address: alexander.mendler@ubc.ca (A. Mendler).

https://doi.org/10.1016/j.ymssp.2023.110783
Received 11 October 2022; Received in revised form 29 April 2023; Accepted 15 September 2023
Available online 25 September 2023

system response to unknown excitation can diagnose damage across the entire structure and under normal operating conditions [4]. Many of them are unsupervised in the sense that, for training, no data is required from the damaged structure. While damage detection can be performed in a purely data-driven fashion [5,6], damage localization is often conducted in combination with numerical models that provide a physical interpretation of the change in the data (in the scope of unsupervised methods), with typical examples being model updating [7], statistical updating [8], parametric change localization [9], and flexibility methods [10]. An overview of recent developments in bridge monitoring can be found in [11]. Diagnostic capabilities beyond localization also require a numerical model of the structure [12], and may only be reliable in combination with non-destructive testing [13].

One group of unsupervised methods that can be evaluated in combination with numerical models are parametric hypothesis tests based on the asymptotic local approach [14], which are capable of detecting and localizing damages [15–20]. The analysis procedure starts with a definition of damage as a change in model-based design parameters, for example, material properties, or cross-sectional values in a finite element (FE) model. Next, parameter changes are linked to changes in the global damage-sensitive features using sensitivity vectors, and uncertainties in the estimation of the data-driven feature are quantified. This way, statistical hypothesis tests, such as the generalized likelihood ratio (GLR), can be applied to test the likelihood of changes in structural parameters. Due to the change linearization through model-based sensitivity vectors, it is possible to analyze vibration data from the undamaged structure and to make predictions regarding the damage *detectability* before damage occurs. In fact, analytical formulas exist to evaluate the minimum detectable damage based on a user-defined probability of detection [21], and to optimize the sensor placement accordingly [22]. As outlined by Falcetelli et al. [23], there is a need to develop similar reliability metrics for damage localization, and the purpose of this article is to present a framework to assess damage *localizability*. Before this can be done, some issues related to damage localization have to be highlighted.

Damage localization is more challenging than damage detection, because changes in features are mapped onto structural parameter changes in FE models (through sensitivity vectors), which introduces the issue of over-parametrization, meaning changes in multiple structural parameters have a similar effect on global damage-sensitive features. Vice versa, it is not possible to identify the very parameter that has changed due to damage, i.e., to localize damage. These issues are well-known in the model updating community [24–26], and typically, method-specific regularization approaches have to be applied to improve the ill-posedness of the localization problem [27]. Alternatively, one of the various methods in the literature [28] can be applied to improve the ill-conditioning by reducing the number of parameters to a smaller subset, including the colinearity index method [29], the column-pivoting method [30], an extension of the relative gain array [31], the Gram–Schmidt orthogonalization [32], principal component analysis [33], or the Fisher information matrix. In the latter case, the trace of the Fisher information is employed, its determinant [34], singular values [35], or the matrix inverse [36]. The advantage of the Fisher information is that it accounts for the statistical uncertainties in the features, which discriminates it from other, deterministic approaches, and makes it particularly suited for the parametric hypothesis tests considered in this paper. That is why it was employed in previous publications in combination with k-means clustering or hierarchical clustering [16,20] to remedy the problem of over-parametrization. With this in mind, the attention can be drawn toward the original goal of the paper.

The purpose is to develop criteria to assess damage localizability and to create tools that are universally applicable to a broad range of features, structures, and clustering approaches. For this purpose, the predictive framework for damage detectability [21] is extended to damage localization. However, defining the minimum parameter change for localization tests is not sufficient. While damage detection corresponds to making a 'global' decision on whether or not any parameter changes have occurred, damage localization corresponds to identifying the very parameter that changed, which can be done by applying the statistical tests to each parameter individually. Damage is localized by selecting the parameters that exhibit a test value beyond a safety threshold, but the ambiguity in the test depends on the degree of over-parametrization, and thus, on the parameter clustering. Intuition may suggest to reduce the number of clusters to a minimum to minimize possible false alarms in unchanged parameters, but this smears the damage location and significantly reduces the localization resolution, as every parameter includes the spatial information from the FE model. Since various clustering approaches exist that all depend on user-defined hyperparameters, such as the number of clusters, the second goal of this paper is to optimize the damage localizability with an optimal cluster setting. A good performance of the clustering is determined by high damage detectability, high localization resolution, and low false alarm susceptibility, and the optimal solution is considered as a compromise between the three criteria. This way, the optimal cluster settings can be found in an automated manner, and the performance of the damage localization can be analyzed and optimized before damage occurs.

The paper is organized as follows: Section 2 reviews the employed statistical damage localization tests and Section 3 develops different criteria to assess their performance, i.e., the damage localizability. Based on the results, a procedure is presented in Section 4 that optimizes the performance of the damage localization. In Section 5, the approach is applied to a laboratory steel beam followed by the conclusion in Section 6.

2. Statistical damage localization tests

This section recaps statistical tests to localize structural damage. In the following, damage is defined as a change in structural parameters of a finite element model; however, other analytical models that relate structural input parameters to measurable system response quantities could have been used (surrogate models, wave propagation equations, etc.). The parameter changes typically correspond to changes in material properties or cross-section values [37], prestressing forces [38,39], support conditions [40,41], the entire stiffness of subcomponents [26], geometric properties and parameters that describe the system connectivity [42]. The corresponding parameters are stored in a vector $\boldsymbol{\theta} = [\theta_1, \dots, \theta_H]^T \in \mathbb{R}^H$, and damage in a structural component h is defined as a (relative) change in the corresponding parameter θ_h from its reference value θ_h^0

$$\Delta_h = \frac{\theta_h - \theta_h^0}{\theta_h^0}. \tag{1}$$

2.1. Damage hypothesis

In general, structural parameter changes cannot be measured directly, but a parameter-based damage hypothesis can be made to infer parameter changes from data. In the following, it is assumed that the parameters are in their reference state or that they have changed by $\boldsymbol{\theta} - \boldsymbol{\theta}^0$. The corresponding hypotheses are defined as [14]

$$\begin{aligned} H_0 &: \ \boldsymbol{\theta} = \boldsymbol{\theta}^0 \qquad \text{(reference state)} \\ H_1 &: \ \boldsymbol{\theta} = \boldsymbol{\theta}^0 + \boldsymbol{\delta}/\sqrt{N} \quad \text{(damaged state)}. \end{aligned} \tag{2}$$

where $\boldsymbol{\delta}$ is an unknown change vector and N is the number of recorded samples from the tested structural state. Typically, data is not evaluated directly but damage-sensitive features (e.g. signal statistics, modal parameters) are extracted to reduce the amount of data and highlight damages. Damage can be evaluated by comparing the feature vector to its reference value, and evaluating the residual

$$\mathbf{r} = \hat{\mathbf{f}} - \mathrm{E}\left[\hat{\mathbf{f}}^0\right], \tag{3}$$

where $\hat{\mathbf{f}} = [\hat{f}_1, \ \dots \ , \ \hat{f}_{N_f}]^T \in \mathbb{R}^{N_f}$ is the estimated feature vector, $\mathrm{E}(\cdot)$ is the expectation operator, and $\hat{\mathbf{f}}^0$ is the feature vector in the reference state. Assuming that the outputs of a structure under random excitation can be modeled as a stationary stochastic process, and that a sufficiently long measurement record is available (with theoretically $N \to \infty$), the feature's distribution can often be approximated as a normal distribution after proper normalization, i.e., $\sqrt{N}\mathbf{r} \longrightarrow \mathcal{N}(\mathbf{0}, \boldsymbol{\Sigma})$, where $\boldsymbol{\Sigma} \in \mathbb{R}^{N_f \times N_f}$ is the covariance matrix of the residual vector. Applying the damage hypothesis from Eq. (2), the features' distribution in the damaged state can be approximated as Gaussian as well, according to the local asymptotic approach [14], due to the central limit theorem

$$\boldsymbol{\zeta} = \sqrt{N}\mathbf{r} \longrightarrow \begin{cases} \mathcal{N}(\mathbf{0}, \boldsymbol{\Sigma}) & \text{(reference state)} \\ \mathcal{N}(\boldsymbol{\mathcal{J}}\boldsymbol{\delta}, \boldsymbol{\Sigma}) & \text{(damaged state)}, \end{cases} \tag{4}$$

where $\boldsymbol{\mathcal{J}}$ is the Jacobian matrix, i.e., a matrix that holds the first-order derivative of each residual vector entry with respect to each structural parameter θ_h,

$$\boldsymbol{\mathcal{J}} = \left.\frac{\partial E_{\boldsymbol{\theta}}[\mathbf{r}]}{\partial \boldsymbol{\theta}}\right|_{\boldsymbol{\theta}=\boldsymbol{\theta}^0} = \left[\begin{array}{ccc} \frac{\partial}{\partial\theta_1} E_{\boldsymbol{\theta}}[r_1] & \frac{\partial}{\partial\theta_2} E_{\boldsymbol{\theta}}[r_1] & \frac{\partial}{\partial\theta_H} E_{\boldsymbol{\theta}}[r_1] \\ \vdots & \vdots \ \cdots & \vdots \\ \frac{\partial}{\partial\theta_1} E_{\boldsymbol{\theta}}[r_{N_f}] & \frac{\partial}{\partial\theta_2} E_{\boldsymbol{\theta}}[r_{N_f}] & \frac{\partial}{\partial\theta_H} E_{\boldsymbol{\theta}}[r_{N_f}] \end{array}\right]\Bigg|_{\boldsymbol{\theta}=\boldsymbol{\theta}^0}. \tag{5}$$

In this paper, the subspace-based residual vector is considered as a damage-sensitive residual, which is formed based on subspace properties of covariance functions and is shown to be asymptotically Gaussian [15,18]. It should be emphasized that the methods in the following sections are universally applicable to any feature with a Gaussian distribution, for example, residuals based on covariance functions [43] or modal parameters [44,45]. If environmental variables distort the Gaussian assumptions, a data normalization step can be performed first to obtain the desired statistical properties, for example, based on multivariate linear regression, principal component analysis [46], or auto-associative neuronal networks [47], to name a few.

2.2. Damage localization tests

The main idea of damage localization is to test the hypotheses from Eq. (2) individually for each parameter θ_h, and to localize damage by selecting the parameter that exhibits a test value beyond a prescribed threshold. Among the available statistical tests in the literature, two localization tests have been considered in this context, i.e., the *direct test* and the *minmax test* [19,20]. The direct test is straightforward in its implementation but neglects possible changes in the untested parameters, which can lead to significant test reactions for unchanged parameters beyond the prescribed threshold (false alarms). The minmax test is the primary focus of this paper, as it is the more advanced test with fewer false alarms. It evaluates the minimum likelihood of the tested parameter having changed against the maximum likelihood of changes in untested partitions, i.e., untested parameters or clusters. Mathematically, this concept is implemented through a geometrical projection of the residual vector [19,20]. The projection requires the sensitivity matrix to be of full column rank, meaning changes in the damage-sensitive feature can be clearly assigned to the respective structural parameters (i.e., columns in the Jacobian matrix). Due to the large number of structural parameters in FE models, this requirement is generally not given. Therefore, the parameters with similar sensitivity vectors have to be clustered prior to the damage localization. The clustering procedure [20] is recapped in the following paragraphs, where the only two inputs are the sensitivity matrix and the covariance matrix.

In the literature on statistical tests [16,20], sensitivity-based clustering algorithms are described that preserve the statistical properties of the residual from Eq. (4). First, the Jacobian matrix is normalized using the square root-inverse of the covariance matrix

$$\tilde{\boldsymbol{\mathcal{J}}} = \boldsymbol{\Sigma}^{-1/2}\boldsymbol{\mathcal{J}} = \left[\tilde{\boldsymbol{\mathcal{J}}}_1 \quad \dots \quad \tilde{\boldsymbol{\mathcal{J}}}_H\right], \tag{6}$$

and the similarity of all normalized sensitivity vectors $\tilde{\boldsymbol{\mathcal{J}}}_i$ and $\tilde{\boldsymbol{\mathcal{J}}}_j$, denoted through the subscript i and j, is evaluated using the distance

$$d_{ij} = 1 - \frac{|\tilde{\boldsymbol{\mathcal{J}}}_i^T \tilde{\boldsymbol{\mathcal{J}}}_j|}{\|\tilde{\boldsymbol{\mathcal{J}}}_i\| \cdot \|\tilde{\boldsymbol{\mathcal{J}}}_j\|}. \tag{7}$$

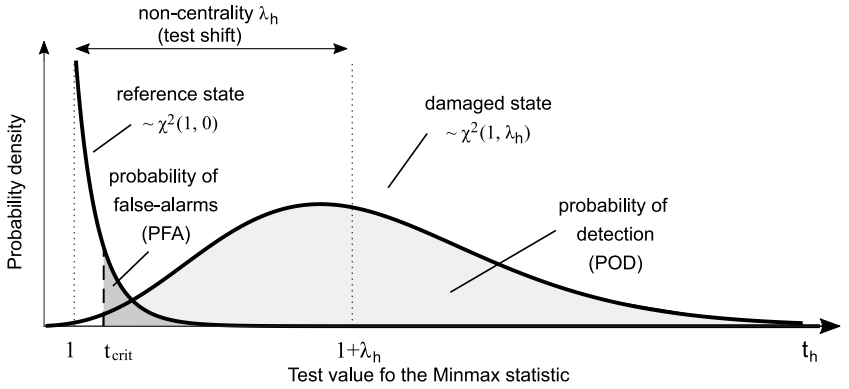

Fig. 1. Statistical distribution of the minmax test statistic from Eq. (12).

If two vectors are orthogonal, the second term (i.e., the cosine of the angle between the vectors) is zero and the distance is maximal with $d = 1$. Two identical vectors lead to $d = 0$. The clusters are formed using, for example, k-means clustering [16] or hierarchical clustering, where the latter has shown to lead to a better performance [20]. In an iterative procedure, the two partitions with the shortest distance are gradually combined until a user-defined distance d_{thres} between clusters is attained. The cluster centers $\mathbf{c}_k$ of each cluster, with $k = 1, \dots, K$ and a maximum number of clusters K, are obtained through averaging

$$\mathbf{c}_k = \frac{1}{m_k} \sum_{i \in C_k} \tilde{\boldsymbol{J}}_i, \tag{8}$$

where m_k is the number of parameters in cluster C_k. Finally, a clustered Jacobian matrix is obtained

$$\boldsymbol{J}^c = \begin{bmatrix} \mathbf{c}_1 & \cdots & \mathbf{c}_K \end{bmatrix}. \tag{9}$$

It is still possible to test the likelihood of changes in individual parameters, not clusters. However, it is not possible to narrow down the damage location within one cluster, as other parameters within the cluster exhibit a significant test shift as well due to their close sensitivities. When testing a parameter θ_h, both the original Jacobian matrix and the clustered Jacobian matrix are evaluated. First, the Jacobian is re-organized as $\boldsymbol{J}_{h,c} = \begin{bmatrix} \boldsymbol{J}_h & \boldsymbol{J}^c_{\bar{h}} \end{bmatrix}$, where the first column $\boldsymbol{J}_h$ is the residual's sensitivity toward the tested parameter and the remaining columns $\boldsymbol{J}^c_{\bar{h}}$ are cluster centers from Eq. (9) except the cluster that contains the tested parameter, denoted as $\mathbf{c}_{k(h)}$, so

$$\boldsymbol{J}^c_{\bar{h}} = \begin{bmatrix} \mathbf{c}_1 & \cdots & \mathbf{c}_{k(h)-1} & \mathbf{c}_{k(h)+1} & \cdots & \mathbf{c}_K \end{bmatrix}.$$

Considering that the clustered Jacobian matrix is already normalized, see Eq. (6), the Fisher information of the partitioned Jacobian matrix can be expressed as

$$\begin{bmatrix} F_h & \mathbf{F}^c_{h\bar{h}} \\ \mathbf{F}^c_{\bar{h}h} & \mathbf{F}^c_{\bar{h}\bar{h}} \end{bmatrix} = \begin{bmatrix} \tilde{\boldsymbol{J}}_h^T \tilde{\boldsymbol{J}}_h & \tilde{\boldsymbol{J}}_h^T \tilde{\boldsymbol{J}}^c_{\bar{h}} \\ \tilde{\boldsymbol{J}}^{cT}_{\bar{h}} \tilde{\boldsymbol{J}}_h & \tilde{\boldsymbol{J}}^{cT}_{\bar{h}} \tilde{\boldsymbol{J}}^c_{\bar{h}} \end{bmatrix}. \tag{10}$$

To implement the minmax test, the Gaussian residual $\boldsymbol{\zeta}$ is projected onto the tested and untested partitions, ζ_h and $\boldsymbol{\zeta}^c_{\bar{h}}$, and a geometrical projection is applied to obtain a robust residual [19]

$$\zeta^*_h = \zeta_h - \mathbf{F}^c_{h\bar{h}} \mathbf{F}^{c-1}_{\bar{h}\bar{h}} \boldsymbol{\zeta}^c_{\bar{h}}, \quad \begin{aligned} \zeta_h &= \tilde{\boldsymbol{J}}_h^T \boldsymbol{\Sigma}^{-1/2} \boldsymbol{\zeta}, \\ \boldsymbol{\zeta}^c_{\bar{h}} &= \tilde{\boldsymbol{J}}^{cT}_{\bar{h}} \boldsymbol{\Sigma}^{-1/2} \boldsymbol{\zeta}. \end{aligned} \tag{11}$$

This operation preserves the residual's information content regarding the tested parameter and makes it blind to changes in untested partitions. Finally, the *minmax test* statistic is defined as

$$t^*_h = F^{*-1}_h \boldsymbol{\zeta}^{*2}_h; \tag{12}$$

it follows a χ^2-distribution with one degree of freedom $\nu = 1$ and a non-centrality λ_h (a mean test shift) of

$$\lambda_h = F^*_h \delta^2_h, \tag{13}$$

where F^*_h is the projected minmax Fisher information

$$F^*_h = F_h - \mathbf{F}^c_{h\bar{h}} \mathbf{F}^{c-1}_{\bar{h}\bar{h}} \mathbf{F}^c_{\bar{h}h}. \tag{14}$$

Damage can be localized by comparing the test statistic t^*_h for each structural parameter θ_h against a safety threshold t_{crit}. This threshold can be set up, for example, based on the relative number of tests beyond the safety threshold in the undamaged state (the

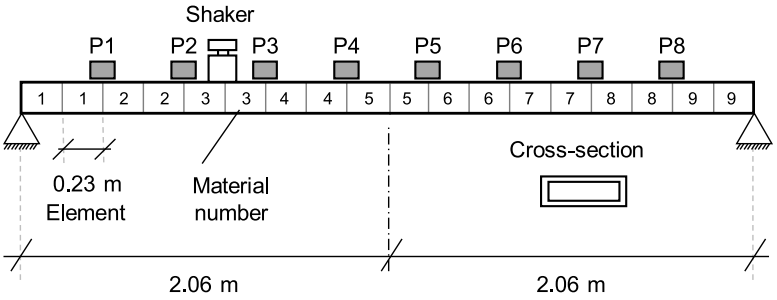

Fig. 2. Finite element model in ANSYS.

Table 1
Parameters for modeling and signal generation.

Structure		Data	
Cross-section	HSS 152 × 51 × 4.78 mm	Measured quantity	Acceleration
E-Modulus	210.000 MPa	Sampling frequency	330 Hz
Density	7.850 kg/m^3	Reference data length	110 min
		Training/testing data	110 min

false alarm rate). The distribution properties are summarized in Fig. 1 together with the safety threshold, and the mean test shift. In the undamaged state, the area under the probability density function beyond the safety threshold is the probability of false alarms (PFA), and in the damaged state, this area is the probability of detection (POD), so finding the ideal threshold is a compromise between minimizing the PFA and maximizing the POD. Note that as the mean test shift increases, the POD increases as well.

Originally, the minmax localization test was designed to eliminate test shifts for unchanged parameters [19], yielding in theory $\lambda_h = 0$ when $\theta_h = \theta_h^0$ in Eq. (13). However, false alarms cannot be excluded if the clustering is not "perfect" in the sense that the number of clusters is not well chosen with respect to their discriminability. So far, no guidance is given on how to set the user-defined threshold d_{thres} and to choose the optimal number of clusters. Furthermore, inaccuracies may arise when the cluster centers are not representative of the contained parameter sensitivities. These issues are the motivation to develop mathematical criteria and predictive methods to assess and optimize the clustering for optimal damage *localizability* in this paper.

2.3. Steel beam case study

To illustrate the statistical localization test from Section 2.2, a numerical case study is presented in this section. The examined steel beam has a length of 4.11 m and a hollow structural steel cross-section (HSS152 × 51 × 4.78) with a total weight of 56.8 kg. It is supported on two pin supports and bent about the weak axis, see Fig. 2. The instrumentation consists of an input source with a total mass of 3.6 kg, as well as eight vibration sensors with a weight of 1.28 kg each, see Fig. 2. The input is a white noise signal and the output is the acceleration in the vertical direction. The beam is used for several case studies [21,22], but in this paper, only the vibration data at sensor positions P1, P2, P7, and P8 are used. All other relevant parameters and signal processing parameters are summarized in Table 1.

Using ANSYS, the beam is discretized into 18 FEs, and to reduce the number of damage scenarios to nine, the same material properties are assigned to two consecutive FE. The instrumentation is considered through point masses that are arranged according to Fig. 2. For the sensitivity computation (of the subspace-based residual), only the first four modes of vibration in the vertical direction are considered, with natural frequencies of 8.8 Hz, 34.5 Hz, 79.6 Hz, and 141.3 Hz, and a modal damping ratio of 1.0% critical damping. The sampling frequency is set to 330 Hz to capture the highest frequency of interest, see Table 1. In the training state, where the sensitivity and the covariance matrix are estimated, the entire measurement record of 110 min is evaluated. In the testing state, the record is split into 100 data segments of 32 s length. Damage is defined as a change in mass, so the monitoring parameters are the nine segment masses of the beam. For the minmax localization test, seven parameter clusters from the above routine are obtained, where the two parameters near the supports are combined to clusters. That means parameters $\{\theta_1, \theta_2\}$ are in the same cluster and changes between them cannot be distinguished, and the same is true for the parameters $\{\theta_8, \theta_9\}$.

For comparison, the localization result for two damage scenarios with extra masses on beam segment 1 and 4 are shown in Fig. 3. The figures show the averaged test values after the extra masses have been applied and 100 test statistics have been evaluated. For the change in segment 1, Fig. 3 (left), a false localization alarm occurs for parameter θ_3 although this test was specifically designed to suppress false localization alarms. Note that parameter 2 is in the same cluster as parameter 1, so the test shift for parameter 2 is consistent with the theory and not considered a false alarm. Possibly a different cluster setting would have fully suppressed the false localization alarm. For the change in segment 4, Fig. 3 (right), the test behaves as expected with no false alarms.

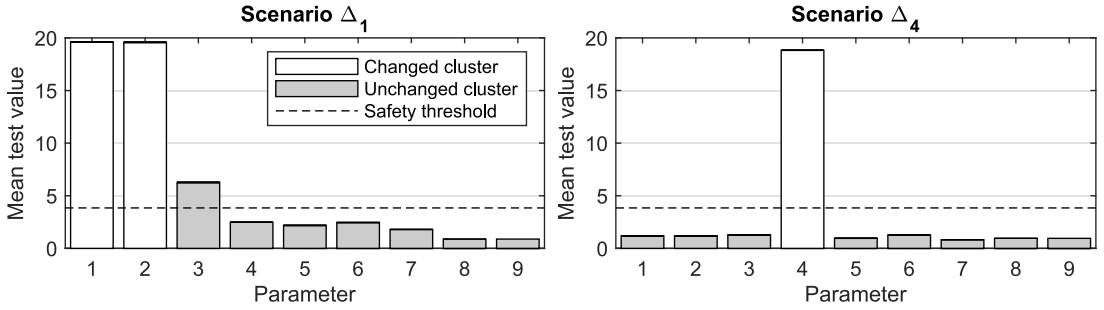

Fig. 3. Mean of the minmax localization test statistic for two selected damage scenarios and numerical data.

3. Criteria for damage localizability

The previous section recapped how statistical tests can identify structural parameters θ_h, $h = 1, \dots, H$ that are most likely to have changed based on information obtained from measurement data. This section goes one step further and develops mathematical criteria to assess the localizability of damage. The most important aspect is a reinterpretation of the formula for the mean test shift from Eq. (13), which allows one to predict the mean test shift based on the respective parameter change. To ease the interpretation and circumvent the combinatorial problem, it is assumed that damage is restricted to a single parameter $\theta_{h'}$, while the other parameters remain unchanged in the following derivations.

3.1. Mean test shift

This section proposes a formula to compute the mean test shift in changed or unchanged parameters. When the parameter is tested for damage that has actually changed, denoted with an apostrophe $\theta_{h'}$, the statistical change vector from Eq. (2) simplifies to $\delta_{h'} = \sqrt{N}(\theta_{h'} - \theta^0_{h'})$ and Eq. (13) turns into $\lambda_{h'} = F^*_{h'}\delta^2_{h'}$. For the unchanged parameter θ_h, with $h \neq h'$, the change vector is $\delta_h = 0$ but the mean test shift λ_h can be unequal to zero. For damaged ($h = h'$) or undamaged ($h \neq h'$) components, the mean test shift can be quantified through one equation

$$\lambda_h = F^{sc}_h(\theta_{h'} - \theta^0_{h'})^2 N, \tag{15}$$

as shown in the Appendix, where the sample size $N = T f_s$ is the product of the measurement duration during testing and the sampling frequency, and F^{sc}_h is the Fisher information after clustering

$$F^{sc}_h = \begin{cases} F_h - \mathbf{F}^{\mathrm{c}}_{h\bar{h}}\mathbf{F}^{\mathrm{c}-1}_{\bar{h}\bar{h}}\mathbf{F}^{\mathrm{c}}_{\bar{h}h} & \text{for} \quad h = h' \\ (F_{hh'} - \mathbf{F}^{\mathrm{c}}_{h\bar{h}}\mathbf{F}^{\mathrm{c}-1}_{\bar{h}\bar{h}}\mathbf{F}^{\mathrm{c}}_{\bar{h}h'})^2/(F_h - \mathbf{F}^{\mathrm{c}}_{h\bar{h}}\mathbf{F}^{\mathrm{c}-1}_{\bar{h}\bar{h}}\mathbf{F}^{\mathrm{c}}_{\bar{h}h}) & \text{for} \quad h \neq h'. \end{cases} \tag{16}$$

The main take-away is that Eq. (16) includes the clustered Fisher information, so the mean test shift in Eq. (15) depends on the cluster settings. If the clustering is "perfect", and if an unchanged parameter is tested, the mean test shift for unchanged parameters is zero, because the Fisher information F^{sc}_h in the lower half of Eq. (16) would simplify to zero. This is of course not true if the tested parameter is in the same cluster as the changed one, because all parameters in the cluster of the changed parameter will show some shift. In contrast, if the averaged sensitivities from Eq. (9) are bad approximations of the contained vectors, the cluster centers are chosen inappropriately, so F^{sc}_h is unequal to zero and false alarms occur for undamaged components. In this case, Eq. (15) also predicts the mean test shifts in the undamaged components with $h \neq h'$, meaning, it predicts false alarms.

The formula from Eq. (15) suggests that the mean test shift (in both undamaged and damaged components) is proportional to the Fisher information F^{sc}_h, which can be calculated based on the Jacobian matrix and the covariance matrix from reference data. That means it is possible to predict the mean test shift without data from the damaged structure, simply based on a hypothetical parameter change $\theta_{h'} - \theta^0_{h'}$. This concept allows for a new way of thinking; the test shift is not evaluated based on empirical studies anymore, but with respect to potential damage scenarios.

3.2. Detectable damage

Being able to predict the mean test shift based on the corresponding parameter change in Eq. (15) inevitably leads to the question of how large the mean test shift should be to allow for a reliable damage localization. The main idea is to require the mean test shift to be fixed to some minimum value $\lambda = \lambda_{\min}$, so the distributions of the test statistic are clearly separated from the undamaged ones, and the probability of detection (i.e., the relative number of tests beyond the safety threshold) is close to 100%, see Fig. 1. At the same time, there is no advantage in increasing the mean test shift beyond the minimum value, as the probability of detection cannot increase beyond 100%. In other words, the required mean test shift $\lambda_{\min}$ is a measure for the reliability of the damage diagnosis

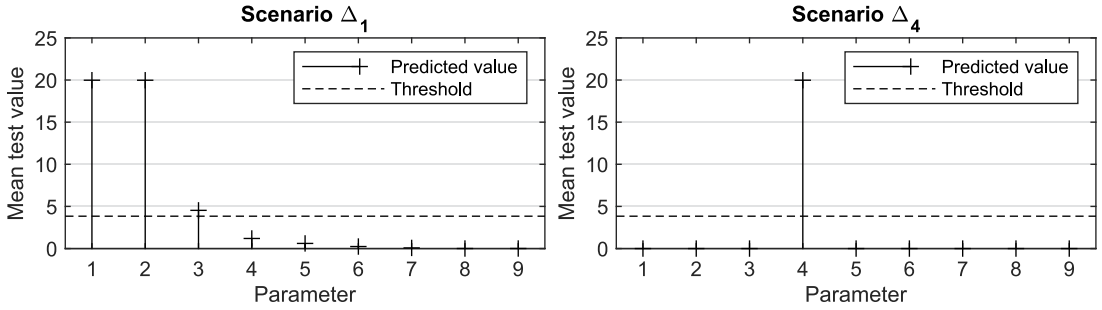

Fig. 4. Predicted mean of the minmax localization test statistic for two damage scenarios and numerical data.

and can be fixed based on the user-defined probability of detection [21]. Once the minimum mean test shift is fixed, the derived formula from Eq. (15) can be solved for the minimum detectable damage in each parameter $\theta_{h'}$

$$\Delta_{h'}^{\min} = \frac{1}{\theta_{h'}^{0}} \sqrt{\frac{\lambda_{\min}}{N \cdot F_{h'}^{sc}}}. \tag{17}$$

High detectability is given for a high absolute magnitude of the design parameter θ_h^0, a high number of samples N, a high Fisher information F_h^{sc} (high sensitivity and a high signal-to-noise-ratio), and low requirements regarding the reliability of the damage diagnosis result, which is achieved by requiring a small mean test shift $\lambda_{\min}$.

3.3. Steel beam case study

For proof of concept, the attention is drawn to the numerical case study from Section 2.3 with the damage localization results in Fig. 3. This time, no vibration data from the damaged structure is evaluated. Based on vibration data from the reference structure, the Fisher information from Eq. (16) is evaluated and the mean test shift for a 5% damage in parameters 1 and 4 is calculated according Eq. (15). For the change in segment 1 (Fig. 4 left), the predicted mean test shift of 20 is identical to the obtained mean test shift from Fig. 3. Moreover, the expected test shift of parameter 2 (in the same cluster) is correctly predicted with a magnitude close to 20, and the false localization alarm of parameter 3 can be quantified based on vibration data from the reference structure. For the change in segment 4 (Fig. 4 right), the predictions also confirm the results from Fig. 3. This illustrates that the experiments based on data from the damaged state are not necessary for the assessment of the mean test shift in changed or unchanged parameters, as the performance of the localization test can be predicted with the developed metrics.

3.4. Definition of localizability

This section proposes several criteria to mathematically define the localizability of damage, with the central element being the formula to predict the mean test shift, Eq. (15). On one hand, the formula can predict the mean test shift for the actually damaged parameter. To clearly detect the damage, the mean test shift has to be beyond a minimum value, specified by the user, and a corresponding parameter change can be calculated. On the other hand, the formula can be used to predict the mean test shift in unchanged parameters, so it is an appropriate tool to assess the magnitude of false localization alarms. Another, rather trivial aspect that affects the localizability of damage is the number of clusters, as this directly affects the localization resolution. In summary, the notion of localizability is defined through the following three aspects:

- Detectability,
- False alarms,
- Resolution.

High localizability is given for a high damage localization resolution, combined with high detectability, and few and insignificant false alarms.

The derived formulas are a powerful tool to analyze the quality of the parameter clustering, as different cluster settings lead to different results for both the detectability and false alarms. To demonstrate this, the mean test shift for a 10% mass change in parameter 2 is plotted in Fig. 5. For a parameter cluster with six clusters (Fig. 5 left) the mean test shift in parameter 2 is about 20, and it reduces to 10 if seven parameter clusters are used (Fig. 5 right). In this particular case, increasing the number of parameter clusters from six to seven eliminated the false localization alarm for parameters 4, 8, and 9, so not only the mean test shift but also the false localization alarms depend on the parameter clustering. The subsequent section will explain how to find the optimal hyperparameters as a compromise between the three criteria.

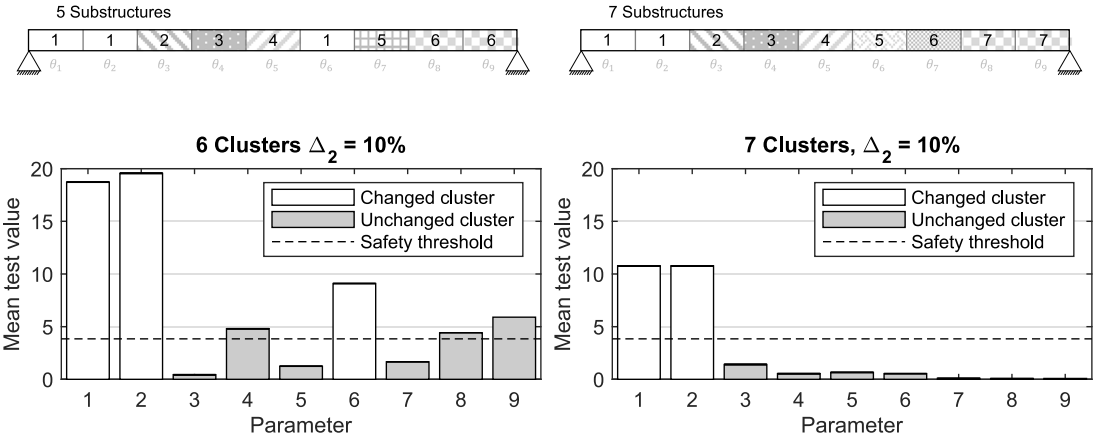

Fig. 5. Mean of the minmax localization test statistic for six clusters (left) and seven clusters (right). Six clusters lead to a high detectability of damage in parameter 2, but seven clusters reduce false alarms.

Table 2
Detectable damage in percent of the structural design parameters for five, seven, and nine parameter clusters.

Detectable damage [%]										
No. of clusters	$\Delta_1^{\min}$	$\Delta_2^{\min}$	$\Delta_3^{\min}$	$\Delta_4^{\min}$	$\Delta_5^{\min}$	$\Delta_6^{\min}$	$\Delta_7^{\min}$	$\Delta_8^{\min}$	$\Delta_9^{\min}$	f_1
5 clusters	21.4	11.6	13.0	11.5	5.8	13.6	12.0	7.0	21.4	21.4
7 clusters	40.6	17.9	13.4	20.4	15.6	15.9	13.8	18.5	42.5	42.5
9 clusters	>100	>100	>100	>100	>100	>100	>100	>100	>100	>100

4. Optimizing the localization performance

The previous section provided a means to evaluate the damage localization performance, which depends on the cluster settings. Based on the three criteria that define the damage localizability, this section outlines a method to find the cluster settings with optimal localizability. In the following, the hyperparameter to be optimized is the number of clusters K in the hierarchical clustering, but the method can be applied similarly to evaluate other cluster settings and approaches.

4.1. Damage detectability

The first criterion is the damage detectability. With increasing number of clusters, the damage detectability in individual parameters decreases, indicated through large minimum damages $\Delta_{h'}^{\min}$. The reason for this is that the minmax localization test considers the maximum likelihood of changes in untested clusters, which naturally increases for an increasing number of clusters. A meaningful way to quantify the detectability of changes is to solve the predictive formula for the minimum detectable damage $\Delta_{h'}^{\min}$, see Eq. (17). After calculating the detectable damage for all parameters $\theta_{h'}$, $h' = 1, \dots, H$, the decisive parameter can be identified as the one with the largest detectable damage $\Delta_{\max}(K) = \max\{\Delta_1^{\min}(K), \dots, \Delta_H^{\min}(K)\}$ as this parameter exhibits the lowest detectability. Subsequently, a weighted optimization criterion can be formed as

$$f_1(K) = \frac{\Delta_{\max}(K) - \Delta_g}{\Delta_b - \Delta_g}, \tag{18}$$

where the subscripts g and b indicate "good" and "bad" values for the detectable damage, or lower and upper bounds in this case. They can be set to, for example, $\Delta_g = 0\%$ and $\Delta_b = 100\%$. Values beyond 100% indicate that damage is not detectable for the given measurement duration.

Example. Table 2 shows the detectable damage for cluster configurations with five, seven, and nine clusters, see Fig. 7. For this specific case, the measurement duration was set to $T = 30\ s$ and the required mean test shift to $\lambda_{\min} = 20$. Looking at the maximum values for each cluster configuration (which corresponds to the objective f_1 for the proposed lower and upper bounds) clarifies that the damage detectability decreases with an increasing number of clusters. For more than seven clusters, the detectable damage exceeds 100%, so damage is not detectable anymore. Note that the parameter changes in Table 2 are not causing the test shifts in Fig. 5. While the figure shows the mean test values of the minmax localization test to an actual change of $\Delta_2 = 10\%$, the table calculates the minimum detectable changes $\Delta_{h'}^{\min}$ based on Eq. (17) such that the user-defined minimum mean test shift of $\lambda_{min} = 20$ is achieved.

4.2. False alarms

The second optimization criterion is the susceptibility to false alarms, which corresponds to a significant test shift for an unchanged parameter that is not in the same cluster as the changed parameter. A test shift for parameters, which are within the same cluster as the damaged component, is to be expected and is not considered a false alarm. As described in the previous section, the magnitude of false localization alarms can be predicted based on Eqs. (15) and (16), and this section explains how to formulate an objective function.

Damage is localized by comparing the test statistic from Eq. (12) against a safety threshold. If multiple parameters exhibit a test value beyond the threshold, damage localization is only reliable if the test shift for changed parameters is more pronounced than for unchanged parameters, especially if only one parameter has changed. Therefore, it is meaningful to evaluate the magnitude of false alarms for all unchanged parameters θ_h, with $h = 1, \dots, H$, in relation to the magnitude of the actually changed parameter $\theta_{h'}$, using the non-centrality ratio

$$\mathrm{NCR}_{hh'} = \frac{\lambda_h}{\lambda_{h'}}. \tag{19}$$

Both the mean test shift for the altered and for the unaltered parameter depend on the parameter change of the actually changed parameter $(\theta_{h'} - \theta^0_{h'})$, meaning the damage extent cancels out and the NCR can be calculated without knowledge of the damage magnitude.

To quantify the susceptibility to false localization alarms for a specific cluster setting, the number of scenarios can be counted, in which false alarms occur. A scenario corresponding to a change in $\theta_{h'}$ is considered a false-alarm-scenario if any NCR from Eq. (19) exceeds a user-defined threshold of, for example, 25%, as higher value may suggest that additional parameters have changed. Moreover, cluster settings that cause NCRs over 100% should be disregarded because it is impossible to identify the correct damage location. Ultimately, an objective function can be formed as

$$f_2(K) = \frac{N_{sc}(K) - N_g}{N_b - N_g}, \tag{20}$$

where N_{sc} is the number of false alarm scenarios, and N_g and N_b are lower and upper bounds that could be set to $N_g = 0$ and $N_b = H$. To penalize settings with high false alarm susceptibility more severely, a lower value for N_b could be chosen.

Example. Fig. 6 summarizes the NCR for the beam from Section 2.3 including all nine damage scenarios. The results are presented for a cluster setting with $K = 7$ clusters and can be interpreted as follows: For scenario Δ_1 (with an extra mass on beam segment 1), the test shift of parameter one is normalized to 100%. Parameter 2 is in the same cluster, so the test shift of close to 100% is not considered a false alarm. Parameter 3 exhibits a false localization alarm, with a significant test shift of 32.4%. Since the false alarms exceed the user-defined threshold of 25% for scenarios 1 and 9, the number of false alarms scenarios is $N_{sc} = 2$, and the objective function is $f_3 = 2/9 = 0.22$.

4.3. Localization resolution

The third and rather trivial optimization criterion is the damage localization resolution. An appropriate measure for the resolution is the number of clusters, because it determines the number of parameters to which changes can be narrowed down. A low number of clusters corresponds to a low localization resolution, and the higher the number of clusters, the higher the resolution. An objective function can be formed as

$$f_3(K) = \frac{K - K_b}{K_g - K_b}, \tag{21}$$

where K is the number of clusters. Damage localization with a single cluster is meaningless, as it merely allows for damage detection, so the lower bound can be set to $K_b = 2$. An upper limit is given through the maximum number of independent sensitivity partitions, best captured through the matrix rank of the Fisher information matrix $K_g = \mathrm{rank}(\mathbf{F})$.

Example. In Fig. 7, the cluster tree (dendrogram) for the steel beam from Section 2.3 is shown, together with the corresponding substructure arrangement for five, seven, and nine clusters. The highest localization resolution with $K = 9$ is achieved if the parameters are not clustered, which is possible because the Fisher information is of full matrix rank, with $\mathrm{rank}(\mathbf{F}) = 9$. It appears that the beam segments close to the supports are combined to parameter clusters first, i.e., parameters $\{1, 2\}$ and $\{8, 9\}$. This is because changes in these beam segments have a similar effect on the global damage-sensitive residual (possibly due to the low vibration amplitudes), which is indicated through a low distance in the cluster tree. Another observation is that, especially for a low number of parameters, clusters are formed for parameters that are not necessarily adjacent to each other. This is an undesired quality because the damage cannot be isolated in one subcomponent. Therefore, it appears intuitive to set the number of clusters to a high value.

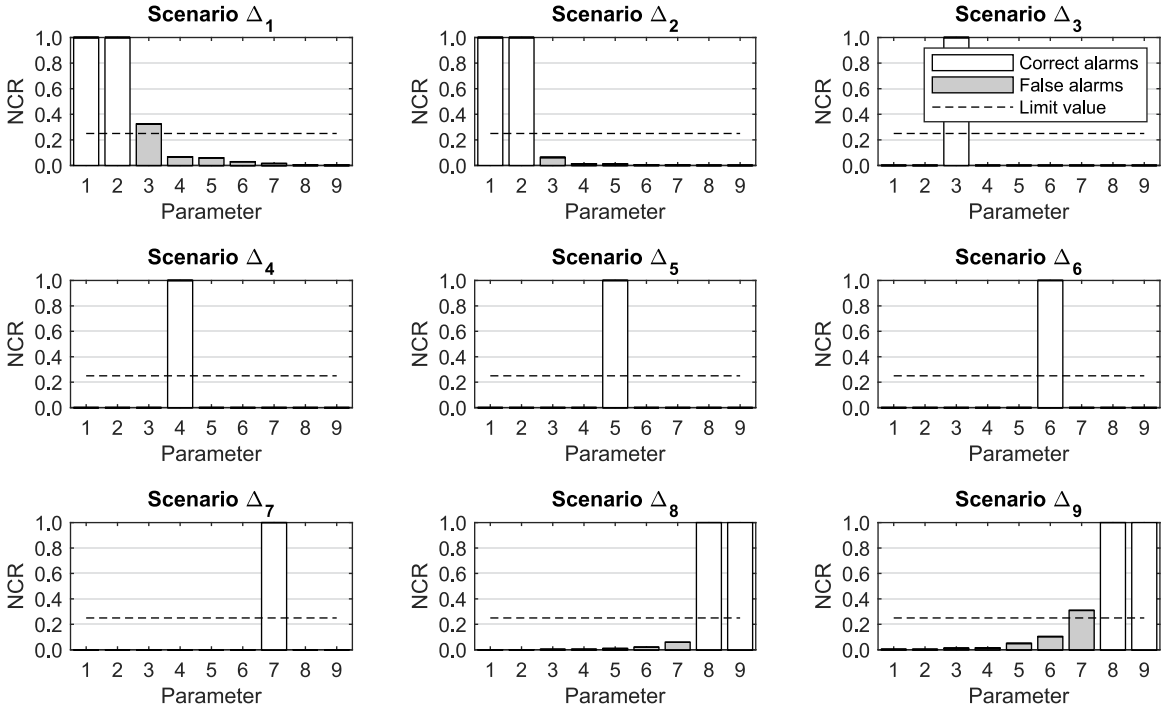

Fig. 6. Non-centrality ratio for all nine damage scenarios.

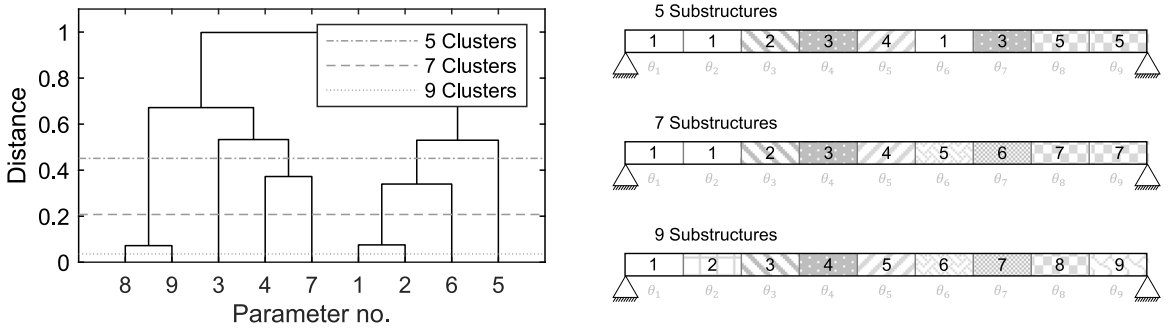

Fig. 7. Cluster tree for pin-supported beam (left) with corresponding substructure arrangement for five, seven, and nine substructures (right).

4.4. Optimal compromise

Finding the optimal hyperparameters is a multi-objective optimization problem. It depends on the damage localization resolution, the damage detectability, and the false alarm susceptibility. After weighing the objective functions using user-defined lower and upper bounds, all criteria are considered equally important. For example, a high damage detectability is useless if the localization resolution is low with $K = 1$, because it is merely possible to detect the presence of damage but not its location. At the same time, a high resolution is meaningless if the false localization alarms are excessive, because the actual damage location remains hidden. Equivalently, a high localization resolution is impractical if damage can only be detected for relative parameter changes close to or beyond 100%. The localization resolution and the damage detectability are conflicting optimization criteria, meaning it is impossible to improve one criterion without degrading the other.

Dealing with conflicting optimization criteria with equal importance is known as Pareto optimization [48]. The optimal solution is the one that simultaneously optimizes the damage detectability from Eq. (18), the false alarm susceptibility from Eq. (20), and the localization resolution from Eq. (21). One way to find the optimal solution is to define a compromise function as the Euclidean distance in the three-dimensional optimization space

$$\begin{aligned} \min_{K} \quad & f = \sqrt{f_1(K)^2 + f_2(K)^2 + f_3(K)^2} \\ \text{s.t.} \quad & f_1(K) < 1, f_2(K) < 1, f_3(K) < 1. \end{aligned} \tag{22}$$

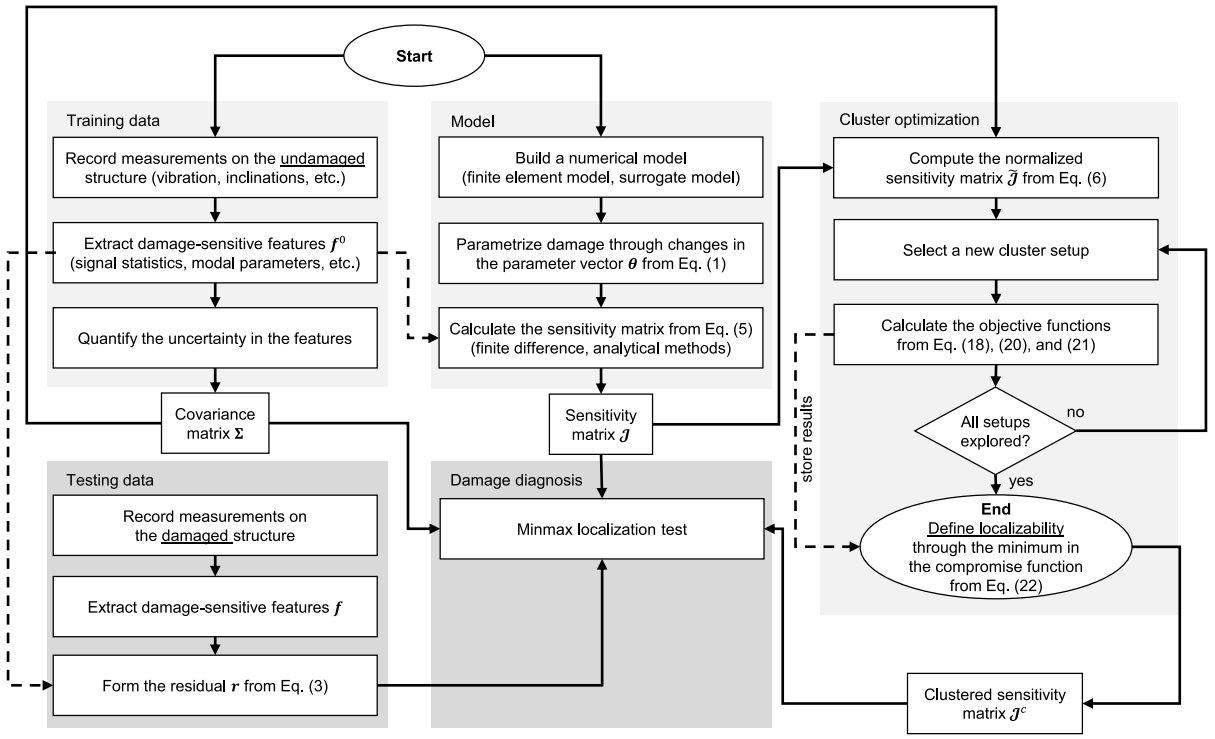

Fig. 8. Flow chart of the optimization scheme, with the final result being the localizability assessment. Light gray boxes indicate that the analysis is based on data from the undamaged structure.

The optimal compromise can then be found by selecting the number of clusters (the localization resolution) with a global minimum in the compromise function f from Eq. (22). To increase the reproducibility, a flow chart is given in Fig. 8.

Example. In Fig. 9, the three objective functions are plotted for a varying number of clusters K. The gray area indicates the infeasible domain, meaning the optimization criterion is beyond the worst value defined by the user, causing the objective function to exceed the value of one. The following observations can be made:

- Damage detectability f_1 (solid black line): Damage detectability is high for a low number of parameter clusters, and gradually worsens with a distinct jump for more than seven clusters. This jump indicates that the detectable damage for the parameters with the lowest damage detectability exceeds 100%, see Table 2.
- False alarm susceptibility f_2 (dotted line): False alarms are zero for one or nine clusters and unequal to zero for most other cases. The allegedly optimal point with seven clusters exhibits an excessive number of false alarms, which underlines the importance of the false alarm susceptibility as an optimization criterion.
- Localization resolution f_3 (dashed line): The worst solution with $f_3 = 1$ is achieved for two parameter clusters, because damage localization with one cluster is meaningless. For an increasing number of clusters, the localization resolution linearly improves.

Fig. 9 also displays the compromise function as a thick, solid black line. A global minimum in the compromise function indicates the optimal compromise between localization resolution, detectability, and false alarm susceptibility. The minimum is reached for $K = 6$ clusters, and the corresponding substructure arrangement is shown in Fig. 10.

All considerations in this section are based on the assumption that the prediction of the mean test shift is accurate. To illustrate this on real data, a laboratory experiment is described in the subsequent section.

5. Experimental validation

For proof of concept, a laboratory steel beam is set up with the same structural properties and signal processing parameters as the numerical case study described in Section 2.3, see Fig. 11. A hydrodynamic shaker (Smartshaker K2007E01) injects white noise excitation vertically into the beam and eight mobile seismic sensors (Tromino tromographs) measure the accelerations in the vertical direction. As in Section 2.3, only the vibration at sensors P1, P2, P7, and P8 are analyzed. The objective is to verify that the optimal cluster setting, which is evaluated based on data from the undamaged structure, actually leads to the optimal damage localization result in the damaged state. For this purpose, a 10% extra mass is applied to two different beam segments (Segment

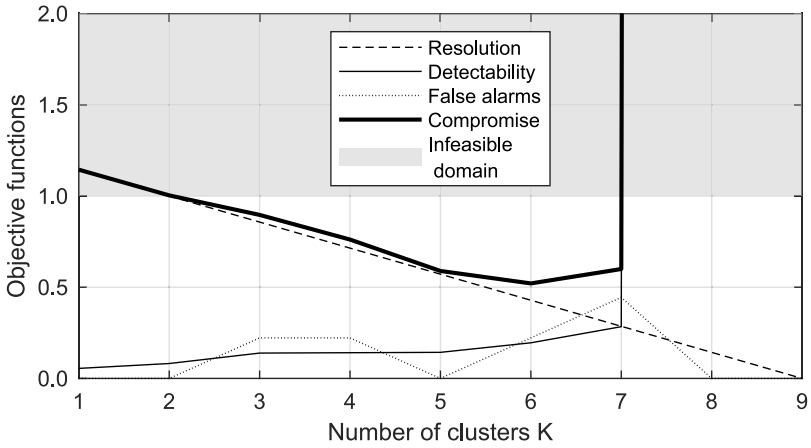

Fig. 9. Objective functions for a varying number of clusters.

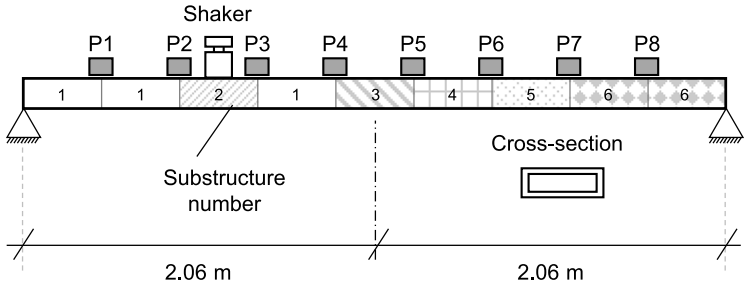

Fig. 10. Optimal substructure arrangement with six parameter clusters.

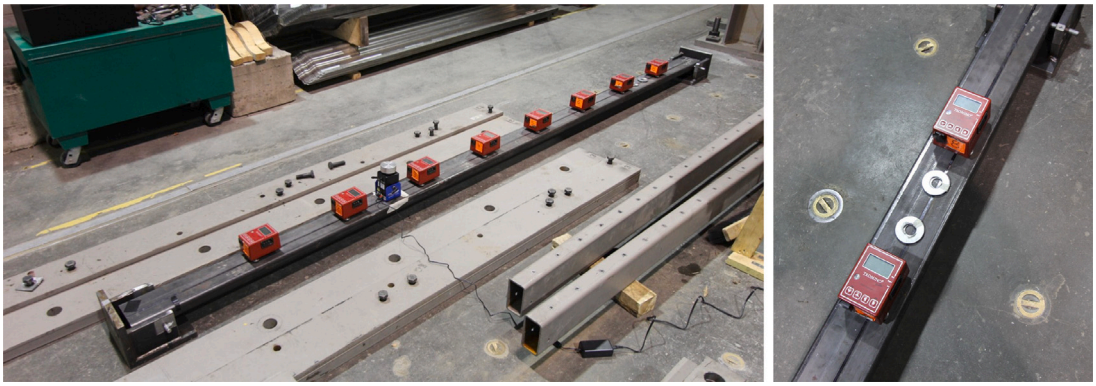

Fig. 11. Photos of the laboratory experiment with a laboratory beam (left) and exemplary extra masses that increase the beam segment weight by 2.5% (right).

5 and Segment 8) and the mean test shift is compared to the predicted values. Based on numerical studies, the accuracy of the predictions has already been validated, as shown in Figs. 3 and 4, and this case study sets out to validate the predictions for a real structure in a laboratory measurement environment. Since real measurement data may have different noise properties (which manifest themselves through the covariance matrix), the results from the automated clustering routine may be slightly different. Hence, all considerations in this section are based on experimental data, including for the undamaged state, and the FE model-based sensitivities.

The results based on numerically generated data indicated that the optimal localization can be achieved for a cluster setting with six parameter clusters, see Figs. 9 and 10. Repeating the analysis from Section 4 and Fig. 8 based on real data leads to an optimal parameter clustering with seven clusters because the covariance properties change and fewer false alarms occur for the cluster setting with seven cluster centers. To validate this allegedly optimal clustering, the test is applied to 100 data sets before and after the extra masses are applied to the beam, in a Monte Carlo experiment. Then, the mean value of the test is determined

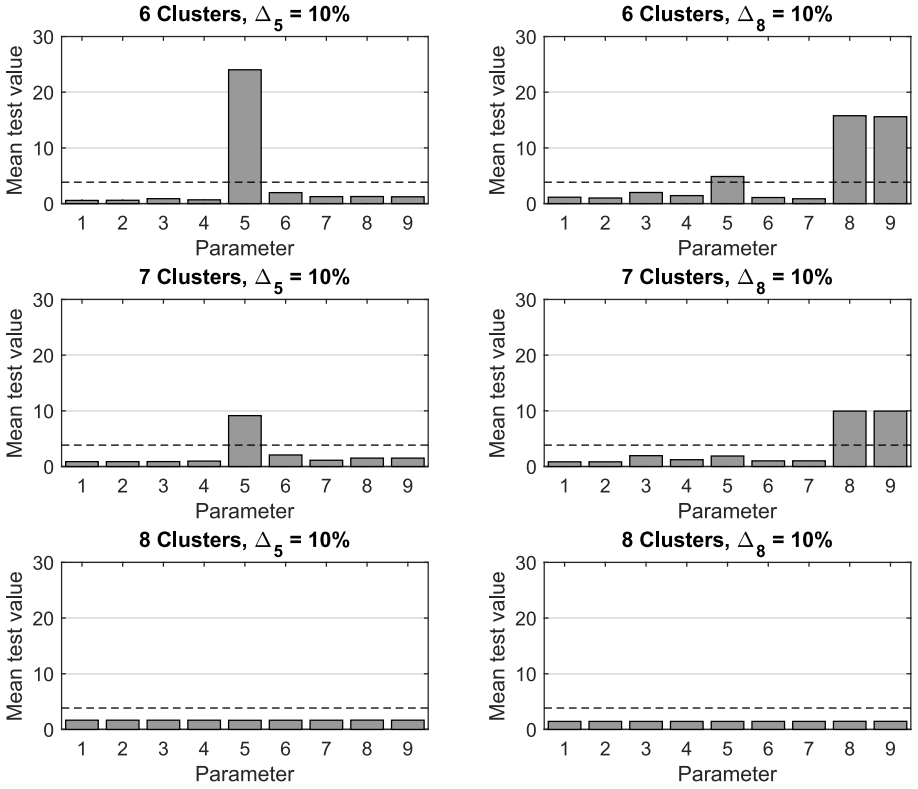

Fig. 12. Mean test shift due to changes in parameter 5 and 8 for a cluster with 6 clusters (top), seven clusters (center), and eight clusters (bottom).

for each monitoring parameter. This analysis is repeated for parameter settings with six, seven, and eight clusters and the results are plotted for both damage scenarios in Fig. 12.

The optimal setup with seven clusters lead to a clear damage localization result, Fig. 12 (center) with mean test values well beyond the safety threshold and no false localization alarms in damage scenarios 5 and 8. For the damage scenario 8, the test shift in parameter 9 was to be expected, as it is within the same cluster as parameter 8, so this is not considered a false alarm. For comparison, Fig. 12 (top) shows the localization result for six parameter clusters. The mean test shift is more pronounced, especially for a mass change in parameter 5. The fact that a lower number of clusters leads to a more pronounced test shift (i.e., a higher detectability) is also represented through objective function f_1 in Fig. 9. Despite the high detectability, the cluster setting with six clusters is sub-optimal because a false localization alarm occurs at parameter 5 for a mass change in parameter 8, Fig. 12 (top right). Increasing the number of clusters to eight, Fig. 12 (bottom), reduces the false alarm susceptibility, but the mean test shift is insignificant in all damage scenarios. This can be tied back to the optimization chart in Fig. 9, as the detectability of damage suddenly decreases and the corresponding objective function enters the infeasible domain, meaning the detectable damage is beyond $\Delta_h = 100\%$.

What remains to be shown is that the test shift cannot only be predicted in relation to other parameters (for the evaluation of false alarms), but that the absolute magnitude of the mean test shift can also be predicted, see Eq. (15). For a 10% mass change in segment 5, six clusters and a measurement duration of $T = 32\,\mathrm{s}$, the predictive formula yields a mean test shift of about $\lambda_5 \approx 20$. By looking at the top left plot in Fig. 12, it can be appreciated that the mean test shift of 23 is very close to the predicted value.

The presented case study demonstrates that the developed optimization scheme leads to optimal damage localization results with high detectability and low false alarm susceptibility. The assumed statistical properties of the damage-sensitive feature and the statistical tests appear to be valid assumptions, even for real structures in laboratory measurement environments. Consequently, it is possible to predict the absolute magnitude of the mean test shift based on vibration data from the undamaged structure and the FE model-based sensitivities. This illustrates the theoretical investigations from Sections 3 and 4, and concludes the validation study.

6. Conclusion

In decades past, extensive research efforts have been made to develop automated systems for damage diagnosis of large structures and ambient vibration data. An aspect that has often been neglected is the proper performance assessment of SHM systems before damage occurs, or possibly, before the structure is instrumented. However, being able to assess the effectiveness of a damage

localization method helps to convince decision-makers of the value of implementing a monitoring system, and being able to optimize the performance may improve the success rate of future monitoring systems. This article demonstrates that the damage localization accuracy with the considered method class (statistical sensitivity-based tests) not only depends on the monitored data-driven features and the complexity of the structure, but on user-defined hyperparameters that are required to overcome the ill-conditioning of the localization problem. The main contributions are:

- A novel framework to analyze the localizability of damages for the considered method class (statistical sensitivity-based tests) based on data from the undamaged structure and sensitivity vectors that are calculated based on numerical models;
- Three mathematical criteria to assess the localizability of damage, i.e., the localization resolution, the damage detectability, and the false alarms susceptibility;
- An automated routine, based on Pareto optimization, to set the hyperparameters of the damage localization procedure, so an optimal localization performance can be achieved as a compromise between maximizing the resolution, maximizing the detectability, and minimizing false alarms.

From a higher-level perspective, this can be seen as the first attempt to define, and mathematically quantify, the localizability of damage. The approach is specific to the underlying damage localization method, and the case studies focus on the localization of mass changes based on vibration-based damage-sensitive features. However, the approach is universally applicable to other features, damage scenarios, and structures, provided the following requirements of the underlying method class for damage localization [9] are fulfilled:

- Gaussian features: The measured damage-sensitive features can be approximated with a Gaussian distribution. This is the case for various vibration-based features, as justified by the central limit theorem from Eq. (4). If environmental and operational variables distort the Gaussian distribution, the method is still applicable if appropriate data normalization steps are performed first, e.g., based on multiple linear regression or principal components analysis.
- Linear models: The relation between changes in structural parameters and measurable features can be linearized using a first-order Taylor series expansion. This is usually valid for small structural changes, or semi-log or log–log scales.
- Calibrated models: The numerical model (e.g. finite element model or other models that relate changes in structural parameters to changes in measurable response quantities) has to be calibrated for a physically meaningful damage localization.

The last requirement may be restrictive for disciplines with complex engineering models, such as bridge, maritime, or aerospace engineering. Therefore, future research should focus on how to incorporate the modeling uncertainty in the predictive framework, as well as application of the methodology to full-scale structures in the field of structural health monitoring, or complex laboratory specimen in the field of non-destructive testing. The presented method was developed to assess the localizability of damage before it occurs, but it is also an appropriate tool to optimize all user input parameters. For example, it is shown how to optimize the hyperparameters for clustering in the presented case study. The linkage criterion and other clustering settings remain undiscussed, but the framework could assist in finding the cluster settings that lead to the fewest false alarms. Equivalently, the framework can be utilized to compare various damage-sensitive features and sensor layouts, and to select the most sensitive ones. This will be explored in future research studies.

Declaration of competing interest

The authors declare that they have no known competing financial interests or personal relationships that could have appeared to influence the work reported in this paper.

Data availability

Data will be made available on request

Appendix. Statistical properties of the minmax localization test

This section evaluates the statistical properties of the minmax localization test under clustering and derives a Fisher information for both changed and unchanged parameters that are tested. To simplify the notations, parts of the Fisher information matrix are defined as $F_h = \boldsymbol{J}_h^T \boldsymbol{\Sigma}^{-1} \boldsymbol{J}_h$, $F_{hh'} = \boldsymbol{J}_h^T \boldsymbol{\Sigma}^{-1} \boldsymbol{J}_{h'}$, and the parts of the clustered Fisher information matrix are defined in Eq. (10).

For notational convenience, it was assumed that damage is restricted to a single parameter $\theta_{h'}$, i.e., $\mathrm{E}[\boldsymbol{\zeta}] = \boldsymbol{J}\boldsymbol{\delta} = \boldsymbol{J}_{h'}\delta_{h'}$ with $\delta_{h'} = \sqrt{N}(\theta_{h'} - \theta_{h'}^0)$, and the tested and changed parameters are labeled through h and h'. From Eq. (11), the statistical properties of the projected residuals are

$$\zeta_h = \boldsymbol{J}_h^T \boldsymbol{\Sigma}^{-1} \boldsymbol{\zeta} \longrightarrow \mathcal{N}(F_{hh'}\delta_{h'}, F_h), \tag{A.1}$$

$$\boldsymbol{\zeta}_{\bar{h}} = \bar{\boldsymbol{J}}_{\bar{h}}^{cT} \boldsymbol{\Sigma}^{-1/2} \boldsymbol{\zeta} \longrightarrow \mathcal{N}(\mathbf{F}_{\bar{h}h'}^{c}\delta_{h'}, \mathbf{F}_{\bar{h}\bar{h}}^{c}). \tag{A.2}$$

The minmax localization evaluates the minimum likelihood of damage in the tested parameter from Eq. (A.1) against the maximum likelihood of damage in all untested clusters from Eq. (A.2). The result is the robust residual in Eq. (11), satisfying

$$\zeta_h^* = \zeta_h - \mathbf{F}_{h\bar{h}}^{c} \mathbf{F}_{\bar{h}\bar{h}}^{c-1} \boldsymbol{\zeta}_{\bar{h}} \longrightarrow \mathcal{N}(F_{hh'}^*\delta_{h'}, F_h^*), \tag{A.3}$$

where

$$F^*_{hh'} = F_{hh'} - \mathbf{F}^c_{h\bar{h}}\mathbf{F}^{c-1}_{\bar{h}\bar{h}}\mathbf{F}^c_{\bar{h}h'} \tag{A.4}$$

$$F^*_{h} = F_{h} - \mathbf{F}^c_{h\bar{h}}\mathbf{F}^{c-1}_{\bar{h}\bar{h}}\mathbf{F}^c_{\bar{h}h}. \tag{A.5}$$

Note that if the tested and the changed parameter are in different clusters, then $\tilde{\boldsymbol{J}}_{h'}$ should lie in the column space of $\tilde{\boldsymbol{J}}^c_{\bar{h}}$ if the clustering is "perfect", which leads to $F^*_{hh'} = 0$ in this case. Pre-multiplying the square root inverse of the variance to Eq. (A.3) leads to a variable with unit variance

$$z = F^{*-1/2}_{h}\zeta^*_h \longrightarrow \mathcal{N}(F^{*-1/2}_{h}F^*_{hh'}\delta_{h'}, 1) \tag{A.6}$$

so the non-centrality can be calculated as

$$\lambda_h = \mathrm{E}[z]^T\mathrm{E}[z] = \delta^2_{h'} \cdot (F_{hh'} - \mathbf{F}^c_{h\bar{h}}\mathbf{F}^{c-1}_{\bar{h}\bar{h}}\mathbf{F}^c_{\bar{h}h'})^2/(F_h - \mathbf{F}^c_{h\bar{h}}\mathbf{F}^{c-1}_{\bar{h}\bar{h}}\mathbf{F}^c_{\bar{h}h}). \tag{A.7}$$

If the changed parameter is tested, Eq. (A.7) collapses into $\lambda_{h'} = \delta^2_{h'}F^*_{h'}$.

References

[1] A. Mendler, M. Döhler, C.E. Ventura, L. Mevel, Clustering of redundant parameters for fault isolation with Gaussian residuals, IFAC-PapersOnLine 53 (2) (2020) 13727–13732.
[2] C.R. Farrar, S.W. Doebling, D.A. Nix, Vibration–based structural damage identification, Phil. Trans. R. Soc. A 359 (1778) (2001) 131–149.
[3] A. Rytter, Vibrational Based Inspection of Civil Engineering Structures (Ph.D. Thesis), Aalborg University, Aalborg, 1993.
[4] S.W. Doebling, C.R. Farrar, M.B. Prime, D.W. Shevitz, Damage Identification and Health Monitoring of Structural and Mechanical Systems from Changes in Their Vibration Characteristics: A Literature Review, Tech. Rep. LA-13070-MS512, Los Alamos National Lab., Los Alamos, United States, 1995.
[5] D.C. Montgomery, Introduction to Statistical Quality Control, sixth ed., John Wiley & Sons, Jefferson City, United States, 2007.
[6] O. Avci, O. Abdeljaber, S. Kiranyaz, M. Hussein, M. Gabbouj, D.J. Inman, A review of vibration-based damage detection in civil structures: From traditional methods to Machine Learning and Deep Learning applications, Mech. Syst. Signal Process. 147 (2021) 107077.
[7] M. Friswell, J.E. Mottershead, Finite Element Model Updating in Structural Dynamics, Springer Science & Business Media, Dordrecht, Netherlands, 1995.
[8] E. Simoen, G. De Roeck, G. Lombaert, Dealing with uncertainty in model updating for damage assessment: A review, Mech. Syst. Signal Process. 56 (2015) 123–149.
[9] M. Basseville, L. Mevel, M. Goursat, Statistical model-based damage detection and localization: Subspace-based residuals and damage-to-noise sensitivity ratios, J. Sound Vib. 275 (3–5) (2004) 769–794.
[10] D. Bernal, Damage localization and quantification from the image of changes in flexibility, Mechanics 140 (2) (2014).
[11] Y. An, E. Chatzi, S.-H. Sim, S. Laflamme, B. Blachowski, J. Ou, Recent progress and future trends on damage identification methods for bridge structures, Struct. Control Health Monit. 26 (10) (2019) e2416.
[12] H. Sohn, C.R. Farrar, F.M. Hemez, D.D. Shunk, D.W. Stinemates, B.R. Nadler, J.J. Czarnecki, A Review of Structural Health Monitoring Literature: 1996–2001, Vol. 1, Los Alamos National Laboratory, United States, 2003.
[13] Y. An, E. Chatzi, S.-H. Sim, S. Laflamme, B. Blachowski, J. Ou, Recent progress and future trends on damage identification methods for bridge structures, Struct. Control Health Monit. 26 (10) (2019) e2416.
[14] A. Benveniste, M. Basseville, G. Moustakides, The asymptotic local approach to change detection and model validation, IEEE Trans. Automat. Control 32 (7) (1987) 583–592.
[15] M. Basseville, M. Abdelghani, A. Benveniste, Subspace-based fault detection algorithms for vibration monitoring, Automatica 36 (1) (2000) 101–109.
[16] É. Balmès, M. Basseville, L. Mevel, H. Nasser, W. Zhou, Statistical model-based damage localization: A combined subspace-based and substructuring approach, Struct. Control Health Monit. 15 (6) (2008) 857–875.
[17] M. Döhler, L. Mevel, F. Hille, Subspace-based damage detection under changes in the ambient excitation statistics, Mech. Syst. Signal Process. 45 (1) (2014) 207–224.
[18] E. Viefhues, M. Döhler, F. Hille, L. Mevel, Statistical subspace-based damage detection with estimated reference, Mech. Syst. Signal Process. 164 (2022) 108241.
[19] M. Döhler, L. Mevel, Q. Zhang, Fault detection, isolation and quantification from Gaussian residuals with application to structural damage diagnosis, Annu. Rev. Control 42 (2016) 244–256.
[20] S. Allahdadian, M. Döhler, C. Ventura, L. Mevel, Towards robust statistical damage localization via model-based sensitivity clustering, Mech. Syst. Signal Process. 134 (2019) 106341.
[21] A. Mendler, M. Döhler, C.E. Ventura, A reliability-based approach to determine the minimum detectable damage for statistical damage detection, Mech. Syst. Signal Process. 154 (2021) 107561.
[22] A. Mendler, M. Döhler, C.E. Ventura, Sensor placement with optimal damage detectability for statistical damage detection, Mech. Syst. Signal Process. 170 (2022) 108767.
[23] F. Falcetelli, N. Yue, R. Di Sante, D. Zarouchas, Probability of detection, localization, and sizing: The evolution of reliability metrics in structural health monitoring, Struct. Health Monit. 21 (6) (2022) 2990–3017.
[24] J.E. Mottershead, M. Friswell, Model updating in structural dynamics: a survey, J. Sound Vib. 167 (2) (1993) 347–375.
[25] M.I. Friswell, Damage identification using inverse methods, Phil. Trans. R. Soc. A 365 (1851) (2007) 393–410.
[26] M.I. Friswell, J.E. Mottershead, H. Ahmadian, Finite–element model updating using experimental test data: parametrization and regularization, Phil. Trans. R. Soc. A 359 (1778) (2001) 169–186.
[27] P.G. Bakir, E. Reynders, G. De Roeck, Sensitivity-based finite element model updating using constrained optimization with a trust region algorithm, J. Sound Vib. 305 (1–2) (2007) 211–225.
[28] Y. Chu, J. Hahn, Parameter set selection via clustering of parameters into pairwise indistinguishable groups of parameters, Ind. Eng. Chem. Res. 48 (13) (2009) 6000–6009.
[29] R. Brun, P. Reichert, H.R. Künsch, Practical identifiability analysis of large environmental simulation models, Water Resour. Res. 37 (4) (2001) 1015–1030.
[30] M. Velez-Reyes, G.C. Verghese, Subset selection in identification, and application to speed and parameter estimation for induction machines, in: Proceedings of International Conference on Control Applications, IEEE, Albany, United States, 1995, pp. 991–997.
[31] C.A. Sandink, K.B. McAuley, P.J. McLellan, Selection of parameters for updating in on-line models, Ind. Eng. Chem. Res. 40 (18) (2001) 3936–3950.
[32] K.Z. Yao, B.M. Shaw, B. Kou, K.B. McAuley, D.W. Bacon, Modeling ethylene/butene copolymerization with multi–site catalysts: Parameter estimability and experimental design, Polym. React. Eng. 11 (3) (2003) 563–588.

[33] R. Li, M.A. Henson, M.J. Kurtz, Selection of model parameters for off-line parameter estimation, IEEE Trans. Control Syst. Technol. 12 (3) (2004) 402–412.
[34] S.R. Weijers, P.A. Vanrolleghem, A procedure for selcting best identifiable parameters in calbrating activated sludge model no.1 to full-scale plant data, Water Sci. Technol. 36 (5) (1997) 69–79.
[35] R. Brun, M. Kühni, H. Siegrist, W. Gujera, P. Reichert, Practical identifiability of ASM2d parameters—systematic selection and tuning of parameter subsets, Water Res. 36 (16) (2002) 4113–4127.
[36] É. Walter, L. Pronzato, Qualitative and quantitative experiment design for phenomenological models - A survey, Automatica 26 (2) (1990) 195–213.
[37] J.E. Mottershead, M. Link, M.I. Friswell, The sensitivity method in finite element model updating: A tutorial, Mech. Syst. Signal Process. 25 (7) (2011) 2275–2296.
[38] A. Mordini, K. Savov, H. Wenzel, The finite element model updating: A powerful tool for structural health monitoring, Struct. Eng. Int. 17 (4) (2007) 352–358.
[39] A. Mordini, K. Savov, H. Wenzel, Damage detection on stay cables using an open source-based framework for finite element model Updating, Struct. Health Monit. 7 (2) (2008) 91–102.
[40] A. Teughels, G. de Roeck, Structural damage identification of the highway bridge Z24 by FE model updating, J. Sound Vib. 278 (3) (2004) 589–610.
[41] S. Zhou, W. Song, Updating finite element models considering environmental impacts, in: Proceedings of SPIE 9803, in: Smart Structures and Materials + Nondestructive Evaluation and Health Monitoring, International Society for Optics and Photonics, Las Vegas, United States, March, 2016, p. 98031R.
[42] J. Mottershead, M. Friswell, G. Ng, J. Brandon, Geometric parameters for finite element model updating of joints and constraints, Mech. Syst. Signal Process. 10 (2) (1996) 171–182.
[43] S. Greś, M. Döhler, P. Andersen, L. Mevel, Subspace-based Mahalanobis damage detection robust to changes in excitation covariance, Struct. Control Health Monit. (2021) e2760.
[44] G. Oliveira, F. Magalhães, Á. Cunha, E. Caetano, Vibration-based damage detection in a wind turbine using 1 year of data, Struct. Control Health Monit. 25 (11) (2018) e2238.
[45] S. Greś, R. Riva, C.Y. Süleyman, P. Andersen, M. Łuczak, Uncertainty quantification of modal parameter estimates obtained from subspace identification: An experimental validation on a laboratory test of a large-scale wind turbine blade, Eng. Struct. 256 (2022) 114001.
[46] F. Magalhães, Á. Cunha, E. Caetano, Vibration based structural health monitoring of an arch bridge: from automated OMA to damage detection, Mech. Syst. Signal Process. 28 (2012) 212–228.
[47] H. Sohn, K. Worden, C.R. Farrar, Statistical damage classification under changing environmental and operational conditions, J. Intell. Mater. Syst. Struct. 13 (9) (2002) 561–574.
[48] A. Mesac, Optimization in Practice with MATLAB, Cambridge University Press, Cambridge, United Kingdom, 2015.